SUPPLEMENTARY FIGURE LEGENDS

Supplementary Table S1. Mutation rates in the *LacZ* forward mutation assay.

Supplementary Figure S1. Subunit composition of Pol δ wild type and mutant proteins. 10 pmol of each purified human Pol δ variant was separated on a 4-20% gradient SDS-PAGE gel and stained with Coomassie Blue. Molecular weights are indicated in kDa to the left of the image. The bands correspond to the 125, 66, 50, and 12 kDa subunits; the predicted molecular weight of the tagged 12 kDa subunit is 18 kDa. The band near 30 kDa has been reported to be a degradation product of the p125 subunit (17). The exonuclease-deficient variants contain the D402A substitution.

Supplementary Figure S2. Processivity of purified Pol δ on primed M13 DNA. A. Limiting quantities of the indicated human Pol δ variants were used to extend a singly primed 7.2kb M13 DNA template. The primer was radioactively end-labeled and visualized on a denaturing 14% SDS-PAGE gel. The 3' end of the primer corresponds to M13 DNA position 173. **B.** Termination probabilities for lanes in (A) are shown for each template position. Preferential termination at position 167 is seen, as has been previously reported for this primer-template pair (24).

Supplementary Figure S3. Stimulation of Pol δ variants by PCNA. Wild type, L606G and L606K human Pol δ were utilized to extend poly-dA-oligo-dT in the absence (dark lines) or presence (light lines) of human PCNA as described in Experimental Procedures. The extension time in minutes is indicated on the horizontal axis; the vertical axis indicates the percent of substrate extended after normalizing to the maximally extended wild type Pol δ sample (100% extension refers to wild type Pol δ at 15 minutes in the presence of PCNA). Values are averages from duplicate experiments; error bars indicate the standard deviation.

TABLE I

Mutation rates in the LacZ forward mutation assay

Mispair	Number of detectable sites	WT[a] Number detected	WT[a] Error rate ($x10^{-5}$)	D402A[a] Number detected	D402A[a] Error rate ($x10^{-5}$)	L606G Number detected	L606G Error rate ($x10^{-5}$)	L606K Number detected	L606K Error rate ($x10^{-5}$)
T•dTMP	16	0	0.11	2	1.0	6	14	0	0.13
T•dGMP	27	3	0.19	17	5.1	36	51	8	0.62
T•dCMP	23	0	0.074	5	1.8	12	20	0	0.090
C•dTMP	16	0	0.11	1	0.51	23	55	0	0.13
C•dAMP	25	8	0.54	6	1.9	21	32	2	0.17
C•dCMP	9	1	0.19	0	0.90	0	4.2	0	0.23
G•dTMP	22	0	0.077	4	1.5	21	36	0	0.094
G•dAMP	25	7	0.47	10	3.2	8	12	2	0.17
G•dGMP	19	2	0.18	10	4.3	11	22	1	0.11
A•dAMP	23	4	0.29	13	4.6	27	45	4	0.36
A•dGMP	17	0	0.10	0	0.48	2	4.5	0	0.12
A•dCMP	19	1	0.089	1	0.43	4	8.0	2	0.22
Base Substitutions	125	26	0.35	69	4.5	171	52	19	0.32
+1 Insertions	199	9	0.077	30	1.2	47	9.0	5	0.052
-1 Deletions	199	13	0.11	51	2.1	40	7.7	12	0.13
Large Deletions	not defined[b]	3	6.9	13	72	4	149	8	22

[a] Data for WT and D402A are from: Schmitt, M.W., Matsumoto, Y, and Loeb, L.A . (2009) *Biochimie* 91, 1163-1172

[b] The number of detectable sites for large deletions is not defined, therefore mutant frequencies are reported rather than error rates.

Table S1, Schmitt et al.

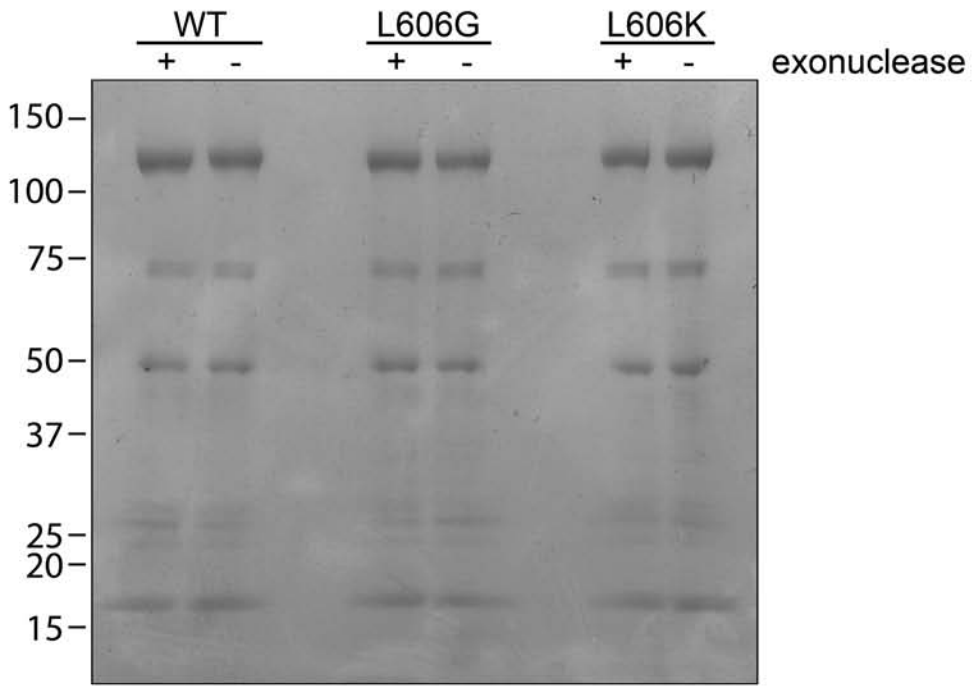

Figure S1, Schmitt et al.

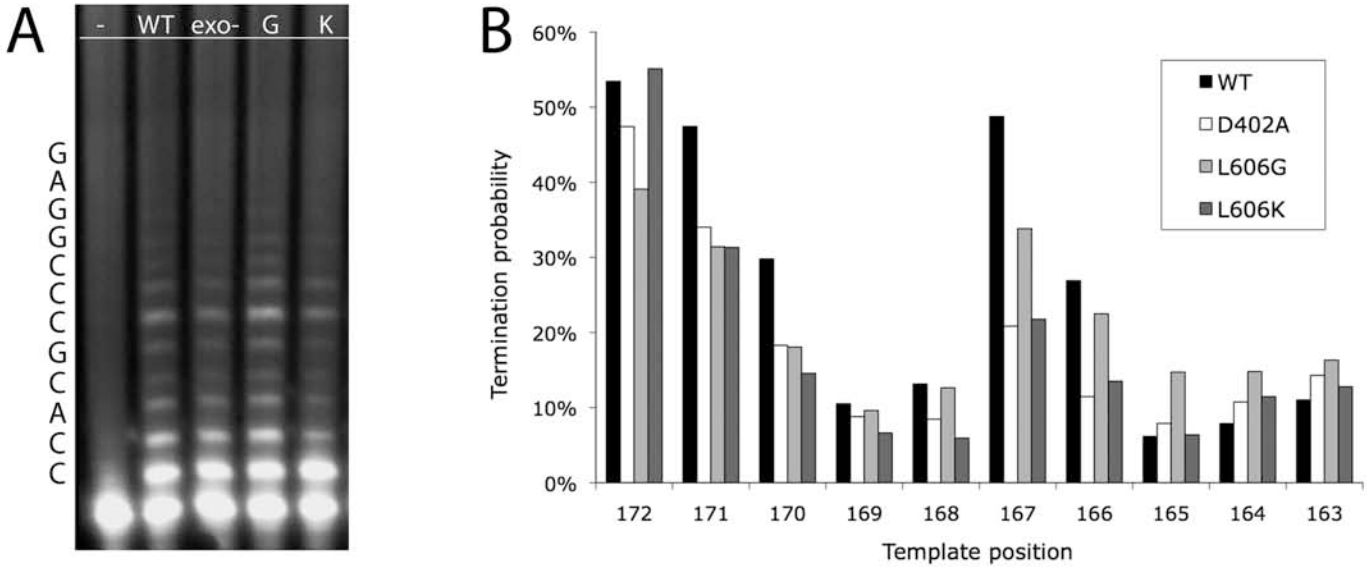

Figure S2, Schmitt et al.

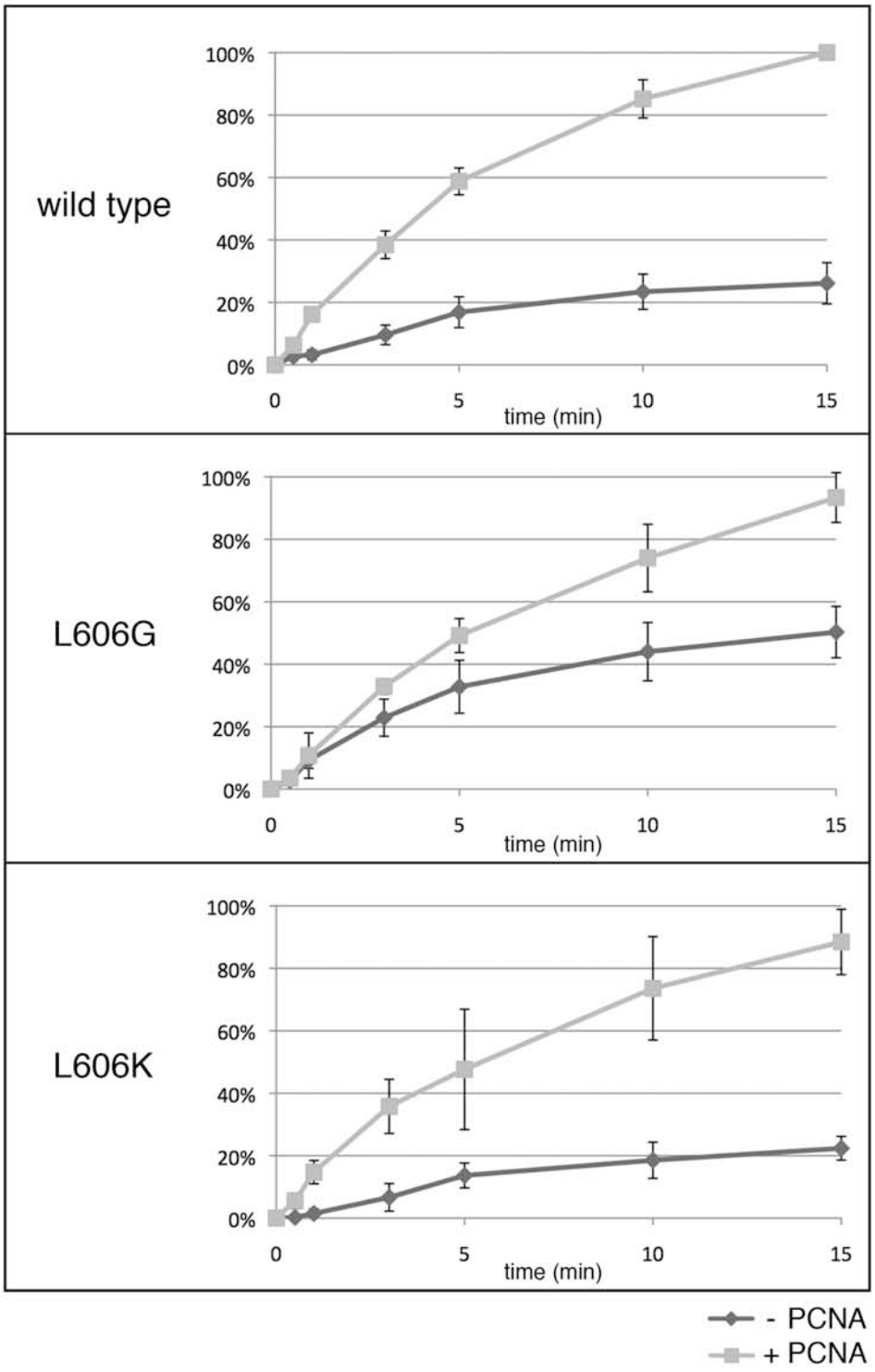

Figure S3, Schmitt et al.